BBA - Bioenergetics 1864 (2023) 148963

Contents lists available at ScienceDirect

BBA - Bioenergetics

journal homepage: www.elsevier.com/locate/bbabio

Proton-translocating NADH:ubiquinone oxidoreductase of *Paracoccus denitrificans* plasma membranes catalyzes FMN-independent reverse electron transfer to hexaammineruthenium (III)

Grigory V. Gladyshev *, Tatyana V. Zharova, Alexandra V. Kareyeva, Vera G. Grivennikova

Department of Biochemistry, School of Biology, Moscow State University, Moscow 119991, Russian Federation

ARTICLE INFO

Keywords:
Bioenergetics
NADH:ubiquinone oxidoreductase (complex I)
Hexaammineruthenium (III)
NADH-OH
FMN
Reverse electron transfer

ABSTRACT

NADH-OH, the specific inhibitor of NADH-binding site of the mammalian complex I, is shown to completely block FMN-dependent reactions of *P. denitrificans* enzyme in plasma membrane vesicles: NADH oxidation (in a competitive manner with K_i of 1 nM) as well as reduction of pyridine nucleotides, ferricyanide and oxygen in the reverse electron transfer. In contrast to these activities, the reverse electron transfer to hexaammineruthenium (III) catalyzed by plasma membrane vesicles is insensitive to NADH-OH. To explain these results, we hypothesize the existence of a non-FMN redox group of *P. denitrificans* complex I that is capable of reducing hexaammineruthenium (III), which is corroborated by the complex kinetics of NADH: hexaammineruthenium (III)-reductase activity, catalyzed by this enzyme. A new assay procedure for measuring succinate-driven reverse electron transfer catalyzed by *P. denitrificans* complex I to hexaammineruthenium (III) is proposed.

1. Introduction

NADH:ubiquinone oxidoreductase (complex I) is the first enzyme complex of mitochondrial and bacterial respiratory chains. It serves as a major electron-entry point for aerobic respiration and thus has a central role in the cell metabolism. Complex I catalyzes oxidation of NADH by ubiquinone coupled to the transmembrane translocation of 4 protons per 2 electrons transferred [1–4], contributing to the formation of proton motive force (*pmf*) across the coupling membrane. It is a very large ~550 kDa protein complex composed of 14 so-called core subunits in bacteria (the minimal composition necessary for the function of the enzyme) [5–9], while *Bos taurus* enzyme consists of 45 subunits – 14 core and 31 supernumerary, and approaches 1 MDa [10–12]. Complex I of *Paracoccus denitrificans*, which is evolutionary related to proto-mitochondria, consists of 17 subunits – it bears 3 supernumerary subunits which have homologs in mitochondrial enzymes [13,14]. Complex I bears a significant number of redox components – noncovalently-bound FMN [15], that serves as the primary electron acceptor for NADH, and 8–9 FeS clusters, depending on the species, that form the redox connection to the terminal acceptor ubiquinone [16,17]. The outstanding advances in determining structures of bacterial, fungal and mammalian complexes I to very high resolutions [18–23] have been recently reviewed by several different groups [24–26]. Interest in the study of complex I has increased in recent years after the discovery of a direct correlation between disturbances of its structure and the occurrence of various pathological conditions of the cell, in particular, the development of certain neurodegenerative diseases and diseases associated with disorders of cellular metabolism [27–30]. The enzyme is also directly involved in ischemia/reperfusion brain injury [31].

Functionally, complex I or its bacterial homologue NADH:quinone oxidoreductase NDH-1 is a fully-reversible enzyme [32] capable of catalyzing reverse electron transfer (RET): reducing NAD^+ by ubiquinol in *pmf*-dependent fashion [33–35]. Such reaction could be observed in coupled membranes when a source for ubiquinol reduction (*e.g.* succinate) and a source for *pmf* generation (*e.g.* succinate or ATP) are both present [33–35]. Besides physiological substrate ubiquinone, complex I reduces a variety of artificial electron acceptors of which ferricyanide (FC) [36] and hexaammineruthenium (HAR), introduced into the

Abbreviations: FMN, flavin mononucleotide; HAR, hexaammineruthenium (III); FC, potassium ferricyanide; NDH-1, bacterial proton-translocating NADH:quinone oxidoreductase; *pmf.*, proton motive force; RET, respiratory complex I-mediated reverse electron transfer; SBPs, plasma membrane particles of *Paracoccus denitrificans*; SMPs, bovine heart submitochondrial particles; Q_1, ubiquinone homologue that has 1 isoprenoid unit in the position 6 of quinone ring; $APAD^+$, 3-acetylpyridine adenine dinucleotide (oxidized); ROS, reactive oxygen species; SOD, superoxide dismutase; PO, peroxidase; AR, Amplex red; BSA, bovine serum albumin..

* Corresponding author.
E-mail address: gg.nurfed@gmail.com (G.V. Gladyshev).

https://doi.org/10.1016/j.bbabio.2023.148963
Received 18 November 2022; Received in revised form 10 February 2023; Accepted 19 February 2023
Available online 24 February 2023

practice in this laboratory [37,38], are the most common. Forward reactions with these substrates are not coupled to proton translocation and are insensitive to the classical inhibitor rotenone [36,37] which binds in the ubiquinone-binding pocket preventing electron transfer to ubiquinone [39]. Reduction of negatively-charged FC proceeds *via* primary electron acceptor FMN [40] and kinetics of NADH:FC-reductase follows a ping-pong bi-bi mechanism and shows a pronounced double-substrate inhibition [36,41]. The reaction with positively-charged HAR is different from that with FC – it doesn't show any substrate inhibition and proceeds *via* a ternary complex mechanism [37,38,42]. Reduction of FC by complex I in RET has also been shown and, as expected, is sensitive to rotenone since electrons are coming from ubiquinol [34]. Another important electron acceptor for Complex I is oxygen which is reduced by the enzyme to produce reactive oxygen species (ROS) both in forward reaction and in RET [43]. Overall, complexes I from different species exhibit very similar kinetic patterns when the same reactions are compared [32,44]. The exception to this is NADH:HAR-reductase activity – when catalyzed by the bovine enzyme at low substrate concentrations it is activated by free (that is, not bound to magnesium ions) ATP by up to 10 times, while the reaction catalyzed by *P. denitrificans* enzyme is unaffected by ATP [45]. Several reviews on complex I activities are available [32,46–48].

A very large number of substances are known to inhibit ubiquinone reduction by complex I, the most commonly used being rotenone and piericidin A [49,50]. On the other hand, only two effective inhibitors competitive with respect to NADH are known, both being NADH derivatives – ADP-ribose (K_i 26 μM for the bovine enzyme) [51] and a pseudo-irreversible NADH-OH (K_i 0.3–10 nM for the bovine enzyme depending on its redox state) [52,53]. Recently, the structure of *Aquifex aeolicus* complex I fragment NuoEF inhibited by NADH-OH was determined at 2 Å resolution [54], unexpectedly showing that nicotinamide ring is opened in this inhibitor which is crucial for its tight binding.

The general consensus in the field right now seems to be that FMN is the only redox group of complex I capable of reducing hydrophilic substances since it's the only matrix-oriented solvent-accessible group judging by structures obtained. Recently we have shown this not to be the case – we observed RET to HAR catalyzed by bovine heart submitochondrial particles (SMPs) and this reaction was insensitive to NADH-OH [55] *i.e.* doesn't involve FMN since it's blocked by the inhibitor. This is a rather striking finding and we wanted to test this further by using different object – coupled plasma membrane vesicles (SBPs) of *P. denitrificans*, especially since it has already shown differences with the bovine enzyme in its interaction with HAR. In this paper we describe in detail the parameters of NADH-OH interaction with *P. denitrificans* complex I and show that it also catalyzes RET to HAR which is insensitive to NADH-OH.

2. Materials and methods

P. denitrificans (strain Pd 1222) cells were grown anaerobically in the presence of succinate and nitrate. SBPs were prepared as described previously [56] with some modifications [57]. The final preparations were suspended (10–15 mg/ml) in 0.25 M sucrose, 10 mM Tris-acetate, pH 7.3, 5 mM Mg-acetate, 1 mM malonate and stored in liquid nitrogen.

Inside-out SMPs of bovine heart mitochondria were prepared, activated, and coupled with oligomycin (0.5 μg/mg protein) as described [58] and stored in liquid nitrogen.

Activities catalyzed by SBPs were assayed in the standard reaction mixture composed of 0.25 M sucrose, 5 mM Tris-Cl^-, pH 8.0, 5 mM $MgCl_2$, 0.2 mM potassium EDTA at 30 °C. The presence of magnesium ions in the reaction mixture is mandatory: it was shown by our group that divalent cations are necessary for the stability of NADH oxidation by SBPs [59]. We brought pH values of additives in aqueous solutions to 8.0 or checked to not change the standard reaction mixture pH. Additions were made in the order specified. Concentrations mentioned for activity assays are final concentrations, unless otherwise stated. Activity values reported were determined as the initial rates, unless otherwise stated. Light absorption was detected with Hitachi-557 spectrophotometer. The rates of NADH oxidation or NAD^+ reduction were detected as absorption changes at 340 nm ($\varepsilon_{340} = 6.22\ mM^{-1}\ cm^{-1}$). The rates of 3-acetylpyridine adenine dinucleotide ($APAD^+$) or FC reduction were detected as absorption changes at 363 nm ($\varepsilon_{363} = 9.1\ mM^{-1}\ cm^{-1}$) or 420 nm ($\varepsilon_{420} = 1.00\ mM^{-1}\ cm^{-1}$), respectively. Production of reactive oxygen species (ROS) was detected as formation of resorufin [60] at 572 nm ($\varepsilon_{572–600} = 54\ mM^{-1}\ cm^{-1}$ as recommended by the suppliers) in the presence of superoxide dismutase (SOD) and horseradish peroxidase (PO) as described previously [61]. Oxygen consumption was detected amperometrically with a covered platinum electrode.

Preliminary membrane energization is required for both succinate-driven and ATP-driven succinate-supported RET (ATP-driven from here on) catalyzed by *P. denitrificans* SBPs. So, succinate-driven RET was measured in the standard reaction mixture at 30 °C after incubation of SBPs with 5 mM succinate for 30 s. The reaction was initiated by the addition of complex I substrate-acceptors (NAD^+, $APAD^+$, FC, and HAR). It is known that *P. denitrificans* SBPs have very low natural ATPase activity [62]. It was shown in our laboratory that this activity is activated by *pmf* [63]. Because of that, to measure ATP-driven RET SBPs were incubated with 5 mM succinate in the standard reaction mixture for 1 min at 30 °C to achieve complete membrane energization and ATPase activation. After that the reaction was initiated by the simultaneous addition of 0.5 mM KCN, 0.5 mM ATP and complex I substrates.

The details of the activity assays are indicated in the Legends to Figures and footnotes to the Tables.

Protein content was determined by the biuret procedure in the presence of deoxycholate using bovine serum albumin (BSA) as a standard.

All data are presented as mean ± SD of at least 3 independent experiments.

Succinate, NAD^+, $APAD^+$, ATP, gramicidin D, rotenone, piericidin A, oligomycin (O-4876), HAR, alamethicin, SOD from bovine erythrocytes (Cat. No. S7571) and from *Escherichia coli* (Cat. No S5639) were from Sigma-Aldrich (USA). NADH and PO (Cat. No. 195372) were from MP Biomedicals (USA). Amplex red (AR) was from AnaSpec, Inc. (USA).

NADH-OH was produced as described by Vranas et al. (Supporting materials and methods in [54]) and purified by ion-exchange chromatography as described originally [52]. Its concentration was determined photometrically ($\varepsilon_{335} = 25\ mM^{-1}\ cm^{-1}$) at pH 12 as described [52]. The resulting preparation (40–60 μM) was aliquoted into small vials and stored in liquid nitrogen. During experiments, the NADH-OH solution was stored on ice. The concentration and stability of NADH-OH was tested by comparing the titers for NADH-OH (0.1 nmol/mg of protein) [53] and for rotenone [64] in NADH:oxidase activity catalyzed by the same SMP preparations. A complete match of these titers indicated the stability of NADH-OH.

Other chemicals of highest purity available were from local suppliers.

3. Results

3.1. Complex I activities in SBPs

Table S1 presents initial rates of complex I-mediated activities catalyzed by *P. denitrificans* SBPs, routinely isolated in this laboratory. These particles show good values of respiratory control (more than 5) without the need of artificial coupling by ATPase inhibitors. They catalyze both the forward *pmf*-generating NADH oxidation and *pmf*-dependent ubiquinol:NAD^+ reduction (RET) at comparable rates. Uncoupled NADH:oxidase can be further stimulated by 1.2–1.5 times depending on the isolated SBPs preparation by the use of channel-forming antibiotic alamethicin. Uncoupled NADH:Q_1-reductase of SBPs was as high as uncoupled NADH:oxidase and more than 85 % rotenone-sensitive which shows the absence of NDH-2 in our

preparation.

Particles prepared were also capable of efficient oxidation of succinate with values of respiratory control of around 2.5. These properties of SBPs enabled us to measure both the succinate-driven RET (where oxidation of succinate provides both ubiquinol and membrane energization) and ATP-driven (where oxidation of succinate provides ubiquinol only, while *pmf* is generated by ATP hydrolysis) to NAD^+ – both reactions showed nearly identical rates and were completely abolished by the addition of uncoupler as expected (see Table S1). In general, all the data reported here on the activities catalyzed by complex I with "physiological" substrates or their analogues demonstrate great reproducibility with the data presented earlier [44].

3.2. Interaction of NADH-OH and complex I in SBPs

To understand whether the hypothetical RET to HAR, catalyzed by *P. denitrificans* SBPs is sensitive to NADH-OH we first had to characterize the interaction between the inhibitor and the bacterial enzyme. NADH-OH is a pseudo-irreversible competitive inhibitor of rat heart [52], bovine heart [52,53] complexes I with respect to NADH. To our knowledge, no data on the interaction of this inhibitor with complex I from *P. denitrificans* has been published. Our null hypothesis was that NADH-OH would bind to the bacterial enzyme with properties very similar to the binding to the bovine one. When uncoupled NADH:oxidase was initiated by the addition of SBPs in the presence of at least a 10-fold excess of NADH-OH (complex I concentration in *P. denitrificans* SBPs was estimated based on the piericidin titer ~0.05 nmol/mg protein [44]) the relatively rapid progress of inhibition was observed (see Fig. 1 A), but to our surprise, the almost complete inhibition was not reached as would have been expected for the bovine enzyme – rather the activity has reached some steady-state level. This conclusion is confirmed by the fact that the dependence of the residual activity of the enzyme upon binding of an excess of the inhibitor in semi-logarithmic coordinates deviates from the kinetics of the pseudo-first order reaction (Fig. 1 D, curve 1).

When a higher concentration of NADH-OH was used then the onset of inhibition was more rapid (compare curves 2, 4, and 5 in Fig. 1 A). Also, when a higher substrate concentration was used the opposite was observed – the onset of inhibition was slower (compare curves 2 and 3 in

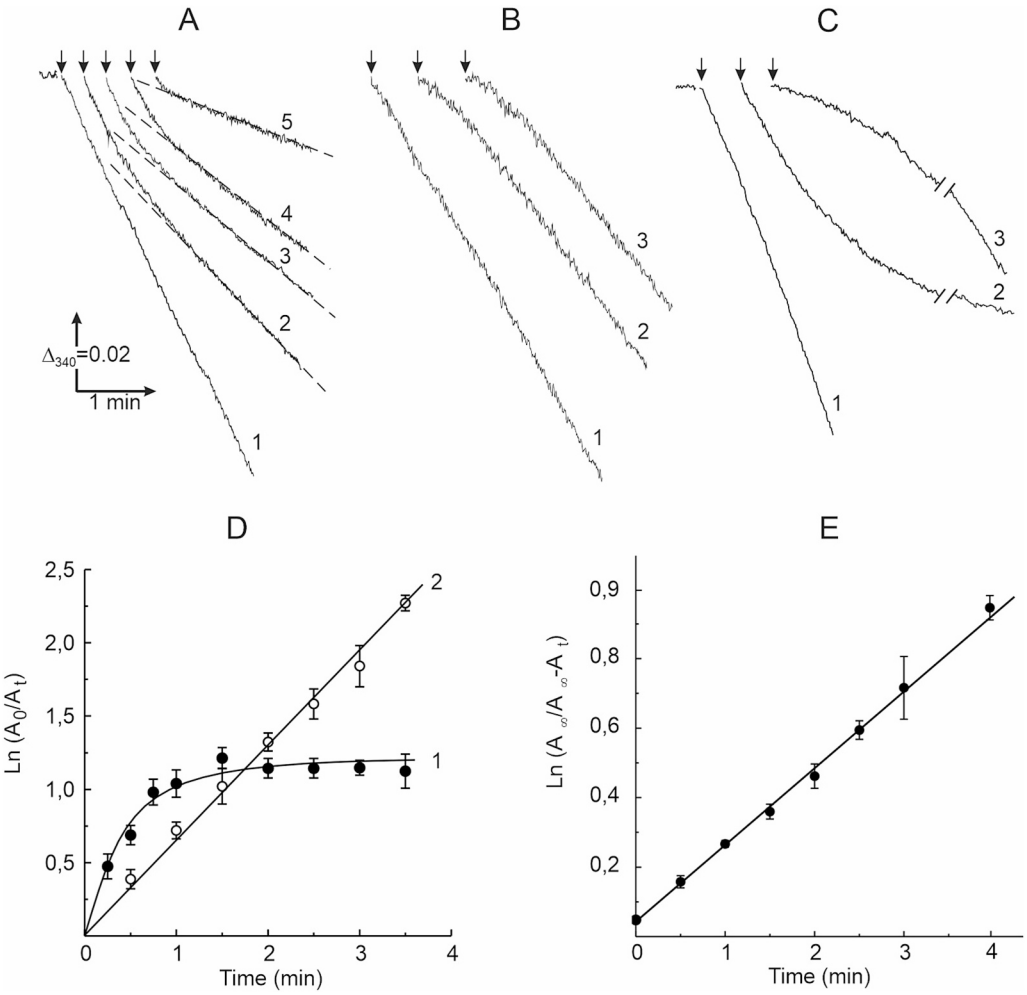

Fig. 1. Inhibition of NADH:oxidase activities of *P. denitrificans* SBPs (A; B; D) and bovine heart SMPs (C; D; E) by NADH-OH. Uncoupled NADH oxidase activity was measured as described in Materials and methods section, in the standard reaction mixture in the presence of 0.0025 μg/ml gramicidin D and 15 mM ammonium acetate. The reaction was initiated by the addition of SBPs or SMPs (10 mg/l, final concentration) (indicated by arrows). (A), actual tracings of the enzyme-inhibitor association. Reaction mixture was supplemented with 75 μM NADH (curves 1, 2, 4, and 5) or 55 μM NADH (curve 3); and 20 nM (curves 2 and 3), or 35 nM (curve 4), or 100 nM NADH-OH (curve 5). Dashed lines indicate the achievement of a *steady-state* reaction rate. (B), actual tracings of the dissociation of the preformed enzyme-inhibitor complexes. SBPs were diluted to 5 mg/ml with the standard reaction mixture and preincubated with 0.25 μM or 2.5 μM NADH-OH (curve 2 and 3, respectively) for 5 min at room temperature and then placed on ice. These particles were then added to the reaction mixture (10 mg/l, final concentration) supplemented with 100 μM NADH. (C), actual tracings of NADH-oxidase activity catalyzed by SMPs in the reaction mixture supplemented with 75 μM NADH in the absence (curve 1, control) and in the presence of 35 nM NADH-OH (curve 2). Curve 3 shows dissociation of the preformed enzyme-inhibitor complex in the reaction mixture supplemented with 100 μM NADH. SMPs (5 mg/ml) diluted in the standard reaction mixture were preincubated with 0.5 μM NADH-OH for 10 min at room temperature and then placed on ice. These particles were then added to the reaction mixture (10 mg/l, final concentration). (D), time-dependence of NADH:oxidase activity during the association NADH-OH with SBPs (●, data from curve 4 in panel A) and SMPs (○, data from curve 2 in panel C) in semi-logarithmic coordinates. A_0 stands for the control activity (no inhibitor in the reaction mixture), and A_t is the residual activity at the time indicated on the abscissa. (E), time-dependence of NADH:oxidase activity during the dissociation of NADH-OH from SMPs in semi-logarithmic coordinates (data from curve 3 in panel C). A_∞ stands for the control activity that would be reached upon the dissociation of enzyme-inhibitor complex, and A_t is the residual activity at the time indicated on the abscissa.

Fig. 1 A). The steady-state activity reached also depended on concentrations of both the substrate and the inhibitor in a fashion expected in the case of competitive binding – higher substrate concentration provided for higher steady-state activity while higher inhibitor concentration provided for lower steady-state activity (Fig. 1 A). This data suggested that NADH-OH is a reversible competitive inhibitor of SBPs with respect to NADH. Next, we preincubated SBPs with different amounts of NADH-OH and then aliquots were withdrawn to measure the residual uncoupled NADH:oxidase: the enzyme-inhibitor complex has apparently considerably dissociated during the time of mixing (around 5 s) not only when the prepared enzyme-inhibitor ratio was around 1:1 (see Fig. 1 B, curve 2), but even when the inhibitor concentration was increased 10 times (see Fig. 1 B, curve 3). Again, after dissociation of the enzyme-inhibitor complex reaction rate reached a constant (steady-state) level (see Fig. 1 B). Note that the apparent *initial rate* of the enzyme-inhibitor complex dissociation practically doesn't depend on NADH-OH concentration. This data suggests that NADH-OH interacts with *P. denitrificans* complex I with a rather high dissociation rate constant (around 1 min^{-1}).

Results obtained differed from our expectations, so we checked inhibition of complex I in bovine heart SMPs by NADH-OH in exactly the same conditions as were used for SBPs (Fig. 1 C). The differences in the inhibition of SBPs and SMPs by NADH-OH can be easily noted when comparing experiments made with the same concentrations of both the substrate and the inhibitor during the association with complex I (compare Fig. 1 A, curve 4, and C, curve 2) as well as the dissociation of the enzyme-inhibitor complex (compare Fig. 1 B, curve 2 and C, curve 3). When uncoupled NADH:oxidase was initiated by the addition of SMPs in the presence of a large excess of NADH-OH, the relatively rapid progress of inhibition was also observed, and after 4 min the residual activity reached the level of less than 10 % of control (curve 2 in Fig. 1 C). Analysis of these data in standard semi-logarithmic coordinates revealed a straight line characteristic of pseudo-irreversible reactions of the first order (Fig. 1 D, curve 2), while for SBPs, a dependence characteristic of reactions coming into equilibrium was obtained (Fig. 1 C, curve 1). SMPs were also preincubated with NADH-OH in 1:1 ratio (complex I concentration was determined based on the NADH-OH [53] and rotenone [64] titers which were equal to 0.1 nmol/mg protein) and then aliquots were withdrawn to measure the residual uncoupled NADH: oxidase activity, which started at almost zero values and progressed to the level of 60 % of control after 4 min, due to slower dissociation of the enzyme-inhibitor complex (Fig. 1 C, curve 3) compared with the dissociation of the bacterial enzyme (Fig. 1 B, curve 2). Thus, the observed transition of NADH-oxidase activity catalyzed by the enzyme in SBPs to the steady-state level can be explained by a higher dissociation rate constant of the bacterial enzyme complex with NADH-OH.

To determine K_i and the rate constants of interaction of *P. denitrificans* complex I and NADH-OH (k_{off} and k_{on}) we came up with a following rationale. If complex I catalyzes NADH oxidation in the presence of a competitive inhibitor – NADH-OH, then the reaction proceeds according to the well-known Scheme 1:

The inhibitor concentration that causes a *steady-state* activity to drop to 50 % of control (IC_{50}) depends on the concentrations of NADH and the inhibitor (NADH-OH), as well as on the K_M of complex I for NADH and K_i

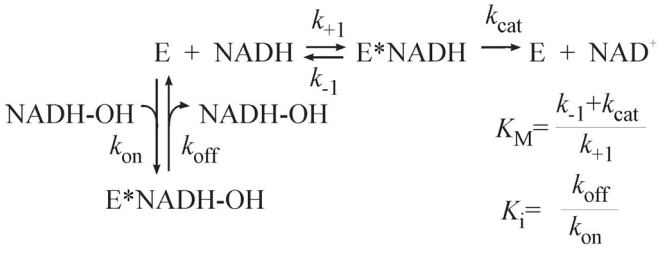

Scheme 1.

for NADH-OH:

$$IC_{50} = ([NADH] + K_M) \times (K_i/K_M) = [NADH] \times (K_i/K_M) + K_i \quad (1)$$

The value of IC_{50} will depend linearly on NADH concentration in the reaction mixture. The intersection with the ordinate axis will give the value of K_i and the slope of this line graph will be equal to K_i/K_M. Thus, the value of the inhibition constant K_i of complex I by NADH-OH can be found.

Fig. 2 A shows the dependences of the residual *steady-state* activities of NADH oxidation on NADH-OH concentration, from which we determined the values of IC_{50}. Those values were plotted as a function of substrate concentration used (Fig. 2 B) and fitted with a straight line. The slope of this line could be established more reliably, so the K_i value of 1.11 ± 0.04 nM was determined from it (the intersection point gives approximately the same K_i value as well). For calculations, we determined the value of K_M for NADH under the same conditions, it was equal to 5.6 ± 0.4 μM. This constant agrees well with the previously reported value of 7 μM [44].

The rate of NADH-OH binding to complex I in accordance with the Scheme 1 for reversible competitive inhibition (see above) is proportional to the fraction of free enzyme E, at any time equal to the ratio $K_M/([NADH] + K_M)$), as well as to the inhibitor concentration. Thus, under conditions of an excess of the inhibitor concentration with respect to the enzyme, the *apparent* pseudo-first order rate constant of the association (binding) k'_{on} will be determined by the equation:

$$k'_{on} = k_{on} \times [NADH - OH] \times (K_M/([NADH] + K_M)) \quad (2)$$

Since NADH:oxidase activity reaches a steady-state rather than complete inhibition in the presence of an excess inhibitor (see Fig. 1 A), an equilibrium between the free enzyme and its complex with the inhibitor is achieved during the steady-state transition, hence the value of the *observed* pseudo-first order rate constant of the association k_{obs} will also include the rate constant of dissociation of E*NADH-OH complex (k_{off}), which is characteristic of first-order *reversible* reactions:

$$k_{obs} = k'_{on} + k_{off} = k_{on} \times [NADH - OH] \times (K_M/([NADH] + K_M)) + k_{off} \quad (3)$$

The binding of the inhibitor to the complex I of *P. denitrificans* can be monitored by a drop in NADH:oxidase activity during the transition from the *initial rate* to the *steady-state phase* of the reaction (for example, see Fig. 1 A, curve 3, and its analysis shown in Fig. 3 A). The linear dependence of the reaction rate on time in semi-logarithmic coordinates, commonly used in the analysis of reversible pseudo-first-order reactions, is shown in Fig. 3 A. From the slope of the straight line, we can find the *observed* rate constant of the pseudo-first order k_{obs}, which in this case was equal to 2.4 min^{-1}. According to Eq. (3), at constant NADH concentration in the reaction mixture and variable concentration of the inhibitor, k_{obs} linearly depends on the NADH-OH concentration, and the slope of the linear graph will be equal to $(k_{on} \times K_M)/([NADH] + K_M)$. If such dependences are obtained at several different concentrations of NADH in the reaction mixture, then a series of straight lines will intersect with the ordinate at one point corresponding to the dissociation rate constant of the enzyme-inhibitor complex (k_{off}). Fig. 3 B shows the results of such measurements.

The dependence of k_{obs} on the inhibitor concentration obtained at several different NADH concentrations was indeed linear and intersected with the ordinate at the same point corresponding to the dissociation rate constant of enzyme-inhibitor complex

k_{off} (0.71 ± 0.07 min^{-1}). From the slopes of these straight lines, we have calculated the value of the second-order rate constant of NADH-OH binding (k_{on}) which turned out to be equal to (7.2 ± 1.3) × 10^8 M^{-1} min^{-1}. Using those values $K_i = k_{off} / k_{on}$ = 0,98 ± 0,21 nM can be calculated. This value agrees very well with the value determined from the graph in Fig. 2 B. This data shows no deviation in NADH-OH interaction with complex I of *P. denitrificans* from a reversible inhibitor competitive with respect to NADH, hence we will consider it like that.

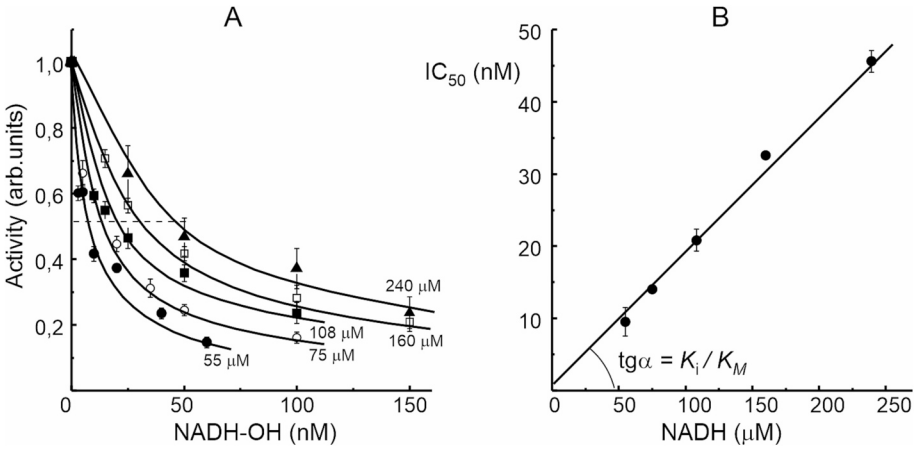

Fig. 2. Determination of the IC_{50} values for the interaction of NADH-OH and complex I in *P. denitrificans* SBPs. Uncoupled NADH:oxidase activity was measured in the standard reaction mixture supplemented with 0.0025 μg/ml gramicidin D, 15 mM ammonium acetate and different concentrations of NADH and NADH-OH. SBPs (10 mg/l) were added to initiate the reaction. (A), the ratios of steady-state activities to the controls at different NADH concentrations (values in μM indicated on the curves) were plotted as a function of the inhibitor concentration. From these dependencies, the IC_{50} values were determined. (B), secondary plot of data shown in panel (A) – IC_{50} values were plotted as a function of NADH concentration to determine K_i for NADH-OH.

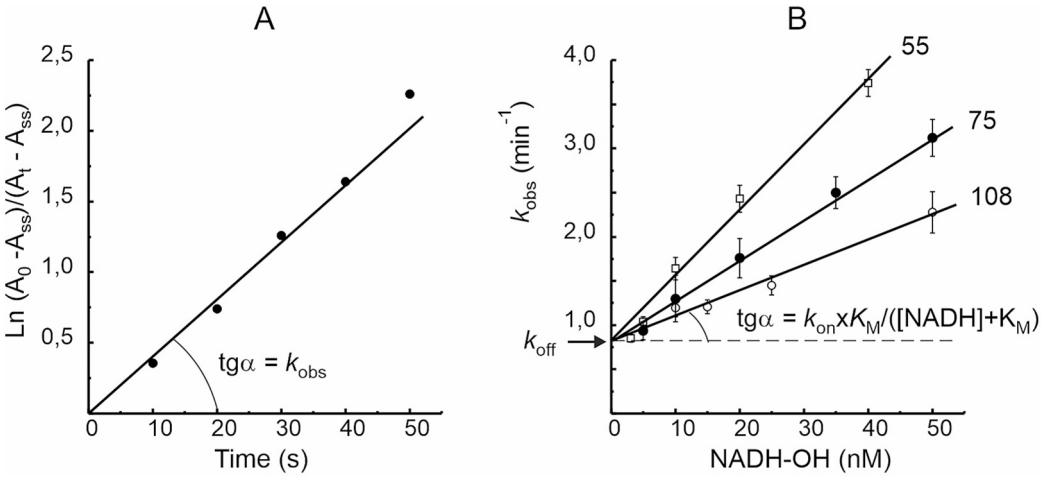

Fig. 3. Determination of the binding parameters of NADH-OH and complex I in *P. denitrificans* SBPs. (A), time-dependence of NADH:oxidase activity during the transition to the steady-state activity in semi-logarithmic coordinates for reversible reactions. A_0 and A_{ss} stand for the control (no inhibitor in the reaction mixture) and the steady-state activities, and A_t is the residual activity during the transition from the initial rate to the steady-state level at the time indicated on the abscissa. (B), dependence of the k_{obs} determined at different NADH concentrations (values in μM indicated on the lines) on the inhibitor concentration.

Parameters of this inhibition seem to be rather peculiar – the inhibitor both binds to the enzyme and dissociates from the enzyme-inhibitor complex rather quickly (in experimental conditions both reactions achieve steady-state in under a minute, see Fig. 1 A and B).

It was of interest to compare the quantitative parameters of NADH-OH binding with complex I from *P. denitrificans* and with complex I from *B. taurus* determined in the same experimental conditions. Since the interaction of the bovine complex I and NADH-OH under conditions of an excess of the inhibitor leads to an almost complete inhibition of the NADH-oxidase activity of the enzyme (Fig. 1 C, curve 2), we used Eq. (2) given on page 12 to determine the second-order rate constant of NADH-OH binding (k_{on}). From the slope of the linear graph shown in Fig. 1 D, we first found the apparent rate constant of the pseudo-first order (k'_{on}) equal to 0.65 ± 0.05 min^{-1}. Then we determined the K_M value for NADH, which under these conditions was equal to 5.5 ± 0.5 μM, as well as the ratio $K_M/([NADH] + K_M)$ (0.07). According to Eq. (2) we have calculated the value of the second-order rate constant of NADH-OH binding (k_{on}) to complex I in SMPs, which turned out to be equal to (0.26 ± 0.02) × 10^9 M^{-1} min^{-1}.

When a preformed 1:1 enzyme-inhibitor complex is diluted by the addition to the standard reaction mixture to initiate the reaction in the presence of saturating concentration of NADH, then the dissociation of inhibitor becomes pseudo-irreversible and could be followed as an increase in NADH:oxidase activity (see Fig. 1 C, curve 3). When that data was analyzed as dependence of the reaction rate on time in semi-logarithmic coordinates, the straight line was obtained (Fig. 1 E). From the slope of this line, the first-order rate constant of NADH-OH dissociation (k_{off}) was determined equal to 0.22 ± 0.01 min^{-1}. Using those values $K_i = k_{off} / k_{on}$ = 0.9 ± 0.1 nM can be calculated. It turned out that K_i values for NADH-OH interaction with both enzymes were comparable (see Table 1), while both rate constants were around 3 times higher for *P. denitrificans* complex I.

Now that the interaction of NADH-OH with *P. denitrificans* complex I was quantified, it was of interest to check RET activities of this enzyme for their sensitivity to this inhibitor. The results are shown in Table S1. Both succinate-driven and ATP-driven RET to NAD^+ and $APAD^+$ were completely sensitive to NADH-OH, corroborating that inhibitor acts on FMN-adjacent nucleotide-binding site. We have also checked succinate-driven RET to oxygen, catalyzed by *P. denitrificans* SBPs (*i.e.* ROS production in RET), which was also completely sensitive to NADH-OH. These results suggest that NADH-OH binding to the enzyme prevents access of very small molecules to FMN.

Table 1
Quantitative parameters of complex I interaction with NADH-OH in the standard reaction mixture (30 °C, pH 8.0).

$k_{on} \times 10^{-8}$ (M^{-1} min^{-1})	k_{off} (min^{-1})	$K_i \times 10^9$ (M)
P. denitrificans SBPs		
7.2 ± 1.3	0.71 ± 0.07	0.98 ± 0.21[a]
		1.11 ± 0.04[b]
B. taurus SMPs		
2.6 ± 0.2	0.22 ± 0.01	0.9 ± 0.1[a]

[a] Calculated as k_{off}/k_{on}.
[b] Determined as in Fig. 2 B.

3.3. RET to HAR catalyzed by SBPs

To find out whether SBPs catalyze RET to HAR, and if so, whether this reaction is sensitive to NADH-OH, we attempted to use the method we developed for measuring ATP-driven RET to HAR in SMPs. Since the reduced HAR formed in this reaction is oxidized by oxygen, RET was evaluated as oxygen uptake under conditions when electron transfer in respiratory chain was blocked by myxothiazol, the inhibitor of complex III [55]. In such conditions, the reoxidation of reduced HAR by oxygen occurs in two ways: *non-enzymatically* as a result of a relatively slow bimolecular reaction, as well as with the participation of cytochrome *c* oxidase, for which reduced HAR is an effective electron donor [65,66]. We have definitely observed HAR reduction in ATP-driven RET catalyzed by SBPs by following the oxygen uptake, but the overall activity was only partially sensitive to uncoupling and piericidin A (data not shown). Two related observations made it problematic to use this technique with SBPs: i) oxygen consumption after the addition of substrates was not linear – apparently it required a buildup of product (reduced HAR), characteristic of the non-enzymatic reaction with oxygen (Fig. S1 shows such a buildup in a model where HAR is reduced by NADH using KCN-inhibited SMPs), which leads us to believe that *P. denitrificans* cytochrome *c* oxidase has lower "affinity" for reduced HAR than the bovine enzyme; ii) it was impossible to find a proper concentration of myxothiazol that completely inhibited respiratory chain of SBPs but didn't affect ubiquinol oxidation by complex I in RET.

So, we decided to find an easily detectable substance that would quickly oxidize reduced HAR even in the presence of oxygen. For this purpose, we tested FC: i) it has a much more positive redox potential than HAR, and ii) FC and HAR have opposite electric charges which may facilitate the reaction between them. To check whether the *non-enzymatic* reaction between reduced HAR and FC is fast enough, so as to effectively preclude reaction with oxygen, we devised the following experiment. To SBPs respiring on NADH as a substrate, KCN was added to block the respiration, after that we added HAR and the oxygen consumption continued – it was caused by the non-enzymatic oxidation of reduced HAR, produced by complex I in NADH:HAR-reductase activity, by oxygen (see Fig. 4, curve 1). When FC was added to the reaction mixture the oxygen consumption abruptly stopped, which indicates that reduced HAR was oxidized by FC, not oxygen, at that moment. After some time, the oxygen consumption continued as expected since all FC added was reduced. One more addition of FC produced the same results. This experiment shows that FC competes quantitatively with oxygen to oxidize reduced HAR. No oxygen consumption besides the reaction on the electrode was detected in the absence of SBPs (Fig. 4, curve 2).

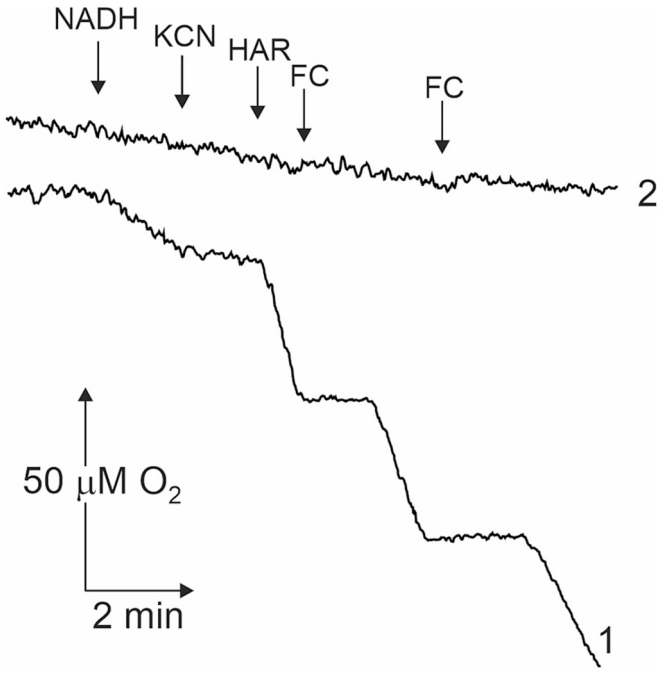

Fig. 4. Amperometric registration of NADH:HAR-reductase activity of *P. denitrificans* SBPs. To the standard reaction mixture supplemented with 200 mg/l SBPs (curve 1) or in the absence of particles (curve 2; non-enzymatic control) the following additions were made (indicated by arrows): 1 mM NADH, 0.5 mM KCN, 100 μM HAR, and 200 μM FC.

Since now we had a tool to measure reduction of HAR in RET using FC as an oxidant for the reduced HAR, we checked whether SBPs catalyze succinate-driven RET to FC and whether it is sensitive to NADH-OH. According to our expectations, FC was indeed reduced by SBPs in succinate-driven RET (Fig. 5 A), and the reaction was only 80 %-sensitive to piericidin A and uncoupling (see Table S1). When SBPs were incubated in the presence of NADH-OH (0.4 μM NADH-OH, 70-fold molar excess of the inhibitor) the rate of RET to FC dropped by about 5 times (Fig. 5 A, compare curves 1 and 2) and the residual NADH-OH-insensitive FC reduction corresponded well to uncoupler- and/or piericidin A-insensitive fraction of this reaction (see Table S1). FC reduction in uncoupler- and/or complex I inhibitor-insensitive residual activity was inhibited by malonate and increased on the addition of KCN (data not shown), which led us to consider this residual activity as succinate: FC-reductase catalyzed by complex II, rather than by complex I. For this reason, we conclude that RET to FC catalyzed by SBPs is fully sensitive to NADH-OH. In the same conditions NADH:HAR-reductase activity was completely blocked by NADH-OH and in the presence of such high concentration of the inhibitor we did not observe its dissociation from the enzyme during the experiment (see Fig. 5 B and Table S1).

To register succinate-driven RET to HAR as catalyzed by SBPs we used following experimental conditions. SBPs were preincubated with NADH-OH to block FC reduction in RET, then succinate was added to energize the membranes and 30 s after that FC was added (Fig. 6 A). The baseline NADH-OH-insensitive FC reduction was recorded and then succinate-driven RET was initiated by the addition of HAR resulting in a considerable increase in the rate of HAR-mediated FC reduction (Fig. 6 A, curve 1). In the absence of SBPs no FC reduction was detected in the assay mixture (Fig. 6 A, curve 2). The only present reductant in the

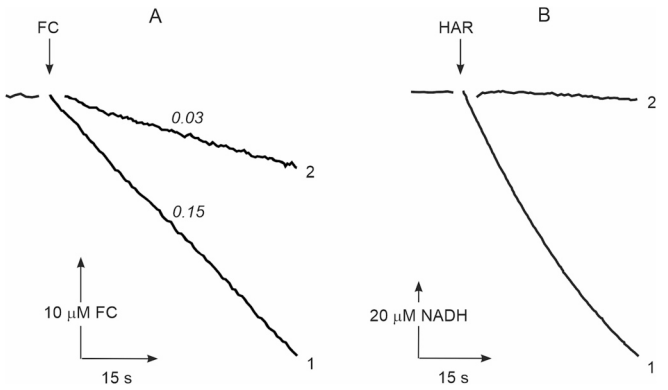

Fig. 5. Inhibition of *P. denitrificans* SBPs-catalyzed activities with artificial electron acceptors by NADH-OH. (A), actual tracings of succinate-driven RET to FC. SBPs (110 mg/l) were incubated in the standard reaction mixture supplemented with 5 mM succinate for 30 s and the reaction was initiated by the addition of 100 μM FC (indicated by an arrow), in the absence (curve 1, control) and in the presence of NADH-OH (curve 2, SBPs were preincubated with 0.4 μM NADH-OH for 3 min prior to the addition of FC). Activity values (2 μē-equivalents/min per mg protein) are shown on the curves; (B), actual tracings of NADH:HAR-reductase reaction. To the standard reaction mixture SBPs (110 mg/l), 0.5 mM KCN and 80 μM NADH were added. The reaction was initiated by the addition of 1 mM HAR where indicated, in the absence (curve 1, control) and in the presence of NADH-OH (curve 2, SBPs were preincubated with 0.4 μM NADH-OH for 3 min prior to the addition of NADH).

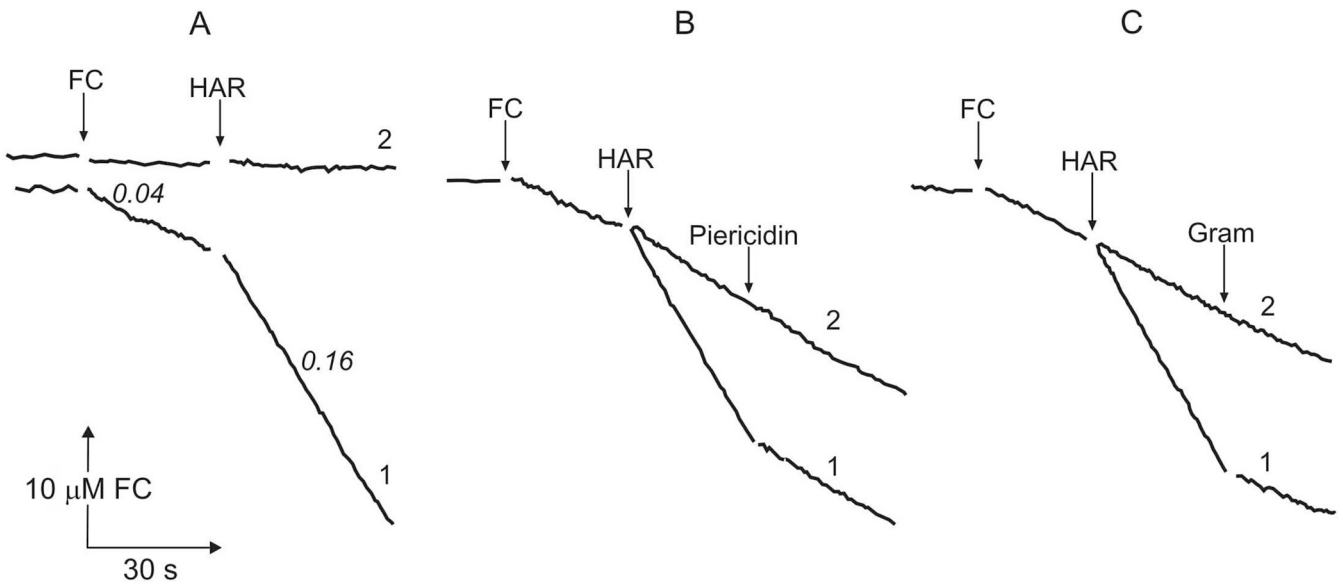

Fig. 6. Actual tracings of succinate-driven RET to HAR catalyzed by *P. denitrificans* SBPs, using FC as a registration system. (A), SBPs (110 mg/l) were incubated in the standard reaction mixture with 0,4 μM NADH-OH for 2.5 min (curve 1; RET to HAR) or no particles and inhibitor were added (curve 2; non-enzymatic control), then 5 mM succinate was added and incubated for 30 s more. After that 100 μM FC and 200 μM HAR were added (indicated by arrows) to initiate the reaction. Activity values (2 μē-equivalents/min per mg protein) are shown on the curves; (B), as in (A), but 2.5 μM Piericidin A was added to the reaction mixture immediately after NADH-OH (curve 2) or where indicated (curve 1); (C), as in (A), but 0.025 μg/ml gramicidin D and 15 mM ammonium acetate were simultaneously added to the reaction mixture 15 s after the succinate addition (curve 2) or where indicated (Gram) by an arrow (curve 1).

system was succinate. So, there are two possibilities for HAR reduction in this system: i) RET to HAR catalyzed by complex I or ii) reduction of HAR by succinate downstream the electron transport chain. To check these possibilities the same activity as shown in Fig. 6 A was measured in the presence of piericidin A. It turned out that when SBPs were incubated with piericidin A or the inhibitor was added during catalysis, the FC reduction rate was lowered back to HAR-independent values (see Fig. 6 B). These results show that HAR-dependent FC reduction is catalyzed by complex I in ubiquinol-dependent manner. Next, the same activity was measured in the presence of an uncoupler that lowered the rate of FC reduction back to HAR-independent values again (see Fig. 6 C). These results show that HAR-mediated FC reduction, catalyzed by complex I in ubiquinol-dependent manner, is also a *pmf*-dependent reaction – *i.e.*, RET. Overall, data shown in Fig. 6 provide direct evidence that complex I in *P. denitrificans* SBPs catalyzes NADH-OH-insensitive succinate-driven RET to HAR with a specific activity of 0,12 2μē-equivalents/min per mg protein (Fig. 6).

3.4. Kinetics of NADH:HAR-reductase activity of complex I in SBPs

FMN is currently considered to be the only redox group capable of reducing hydrophilic electron acceptors. On the other hand, we have demonstrated that complex I in bovine heart SMPs [55] and *P. denitrificans* SBPs (this study) catalyzes RET to HAR, which is

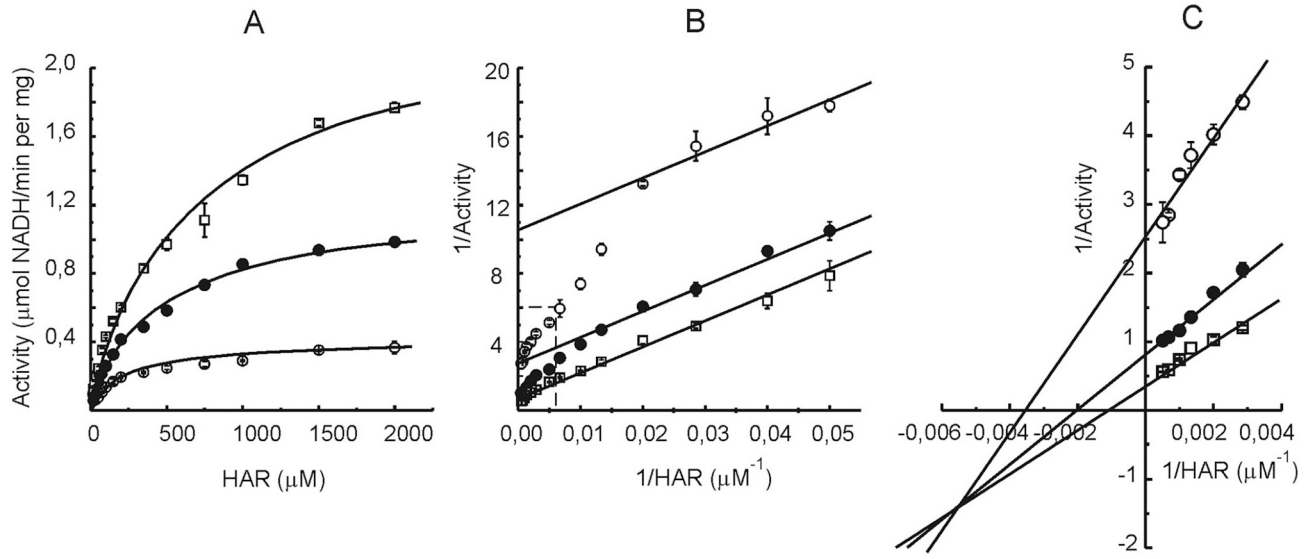

Fig. 7. Initial rates of NADH:HAR-reductase activity catalyzed by *P. denitrificans* SBPs. To the standard reaction mixture SBPs, 5 μM rotenone, 1 mM KCN and different concentrations of NADH were added and the reaction was initiated by the addition of HAR. (A), 5 μM NADH (○), 20 μM NADH (●), 100 μM NADH (□); (B), double reciprocal plot of data shown in panel (A); (C), double reciprocal plot of data at HAR concentrations of 75 μM and higher.

insensitive to NADH-OH. To explain that, we hypothesize that a non-FMN redox could be an electron donor for HAR. If so, the kinetics of NADH:HAR-reductase activity of SBPs should be complex.

To check this, we measured NADH:HAR-reductase activity of *P. denitrificans* complex I in a wide range of substrate concentrations. The results are shown in Fig. 7. This activity increased with an increase in concentrations of both substrates (see Fig. 7 A) but deviated from simple Michaelis kinetics, which can be seen from double-reciprocal plots in a wide range of HAR concentrations (see Fig. 7 B). Data, corresponding to each NADH concentration used, could be roughly extrapolated by two different straight lines in different ranges of HAR concentrations (compare Fig. 7 B and Fig. 7 C; note that the latter graph focuses on higher acceptor concentrations highlighted on graph B by a dashed line). At low HAR concentrations data could be fit by a series of parallel lines (Fig. 7 B), characteristic of ping-pong bi-bi mechanism. At higher acceptor concentrations data is fit with a series of lines intersecting in a third quadrant, characteristic of ternary complex mechanism. From this follows that there are two different kinetic mechanisms of NADH:HAR-reductase activity of *P. denitrificans* complex I (in other words – there are two *kinetically* different electron donors for HAR). Thus, the obtained results corroborate our assumption of FMN-independent pathway for HAR reduction in the reverse electron transfer catalyzed by *P. denitrificans* complex I.

4. Discussion

In recent years, significant progress has been made in the study of the structure of complex I [19–23]. Despite this, all of the proposed mechanisms [23,25,67] for the reaction catalyzed by this enzyme are hypothetical and require rigorous testing. Kinetic studies using various artificial electron acceptors, as well as specific enzyme inhibitors, especially those that bind with a high affinity, remain a useful tool for studying intramolecular electron transfer.

Recently, we have shown that bovine heart complex I catalyzes NADH-OH-insensitive RET to an artificial electron acceptor HAR, and suggested that FMN is not the only redox group of complex I capable of reducing hydrophilic substances [55]. The most important finding reported here is that bacterial complex I is also capable of catalyzing this reaction, thus, suggesting a universality of this phenomenon. Before discussing RET to HAR, we would like to focus in more detail on the interaction of *P. denitrificans* complex I with NADH-OH, a specific inhibitor of the NADH-binding site of the enzyme.

NADH-OH is the only known potent inhibitor of NADH-binding site of complex I. This compound was introduced into laboratory practice by Kotlyar et al. [52], later, the interaction of this inhibitor and the bovine heart enzyme was described in detail [53]. In this work, for the first time, we characterized the parameters of NADH-OH binding to *P. denitrificans* complex I and compared them with those for the bovine enzyme. NADH-OH is a competitive inhibitor respective to NADH of *P. denitrificans* complex I with K_i of 1 nM (Table 1), that is in line with data on bovine complex I, that was also inhibited with the same K_i (Table 1), but it differs significantly from K_i of 46 nM recently determined for *E. coli* enzyme [54]. Despite the close values of the equilibrium inhibition constants for *P. denitrificans* and *B. taurus* enzymes, both *rate* constants (k_{on} and k_{off}) measured in identical conditions were 3 times higher for the bacterial complex I.

Using bovine heart SMPs it was shown that the rate constants of NADH-OH interaction with complex I (k_{on} and k_{off}), as well as K_i, depend on the redox state of the enzyme and differ significantly for the *fully oxidized* and for *reduced* complex I [53]. Currently we cannot answer the question whether *P. denitrificans* enzyme also shows redox-dependent change of nucleotide affinity as does the bovine one, and there is no clear route to finding this out due to the very high rate of NADH-OH dissociation (Table 1).

Recently the structure of *Aquifex aeolicus* complex I fragment NuoEF bound to NADH-OH was determined [54]. The higher affinity of the *A. aeolicus* enzyme to NADH-OH than to NADH comes from two additional strong hydrogen bonds of the inhibitor amide group with conserved $Asp103^F$ and $Glu95^F$ (*A. aeolicus* numbering), additional hydrogen bonding of adenosine pyrophosphate moiety as well as significant shortening of two other hydrogen bonds [54], implying a tight interaction of the inhibitor with NADH-binding site. Higher affinity of NADH-OH to *P. denitrificans* complex I (K_i 1 nM) than to the *E. coli* enzyme (K_i 46 nM) suggests selection of tighter NADH-binding pocket in the course of evolution leading to α-proteobacteria from their common ancestor. It is interesting to note that the difference in NADH-OH affinities is pronounced between the two bacterial enzymes while affinities are nearly the same for the bovine (K_i 1 nM) and *P. denitrificans* complex I. On that basis it could be conjectured that all eukaryotic complexes I should be rather comparable in their affinities to NADH-OH due to their common α-proteobacterial origin. One could also note that even if K_i of *B. taurus* and *P. denitrificans* complex I for NADH-OH are practically equal, the rate constants are lower for the mammalian enzyme, suggesting a higher energy barrier for the binding and hence a further tightening of NADH-binding pocket.

As shown in this study, NADH oxidation and reduction of nucleotides and FC in RET catalyzed by *P. denitrificans* complex I are fully inhibited by NADH-OH (Table S1). Of particular interest are the data showing that NADH-OH completely inhibits ROS generation in RET, catalyzed by the bovine enzyme [61] and *P. denitrificans* complex I (Table S1). All of these results taken together show that binding of NADH-OH in the NADH-binding pocket in close proximity to FMN prevents the electron transfer from FMN and leaves no space even for small molecules (in particular for oxygen) to diffuse to flavin as was demonstrated in the study of the structure of NADH-OH-bound *A. aeolicus* NuoEF fragment of complex I [54]. This conclusion is important for further discussion of the mechanism of the reverse electron transfer to HAR catalyzed by *P. denitrificans* complex I.

NADH:HAR-reductase activity catalyzed by SBPs differs from simple Michaelis kinetics (Fig. 7). It's worth noting that depending on HAR concentration, NADH:HAR-reductase activity proceeds *via* a ping-pong bi-bi mechanism when the acceptor concentration is low, and *via* a ternary complex mechanism at high concentrations of HAR. Two-substrate reactions could follow a ping-pong bi-bi mechanism when the first reaction product (NAD^+) is released before the enzyme interacts with the second substrate (artificial electron acceptor), for example, as in NADH:FC-reductase activity of complex I. More generally, formally the same kinetic behavior can be observed if an enzyme forms a ternary complex with two substrates, but there is an irreversible step in the catalytic turnover. We hypothesize that complex kinetics of NADH:HAR-reductase of SBPs could be expected in a case when there are two different redox components of complex I that are capable of reducing HAR with different apparent parameters. We assume that one of those components is FMN because three-subunit fragment of bovine heart complex I also catalyzes NADH:HAR-reductase activity [38] and analogous two-subunit fragment of *P. denitrificans* was shown to oxidize NADH by both Q_1 and FC [68], while the identity of the second component is not known by us. Midpoint redox potential of FMN in *P. denitrificans* complex I is not known, but was reported for the isolated bovine complex I (from −340 mV to −363 mV at pH 7.5) [69,70]). On the other hand, midpoint redox potentials of four FeS clusters in *P. denitrificans* membranes are more positive, with their values ranging from −285 mV to −160 mV at pH 7.7 (N1b, N2, N3, and N5) [71]. In conditions when NADH:HAR-reductase activity is assayed, electron transfer from FMN to any of these redox centers would likely appear as practically irreversible, since for each ~60 mV of difference in the midpoint redox potentials, the ratio of reduced to oxidized cluster will shift an order of magnitude from that for FMN. Therefore, any of these clusters can be considered as a component donating electrons to HAR. This unidentified redox center reduces HAR at lower concentrations compared to FMN and has a higher “affinity” for the electron acceptor. With an increase in acceptor concentration reduction of HAR by FMN

begins to prevail (lower "affinity" but higher turnover numbers). The latter reaction proceeds *via* the formation of a ternary complex, as was suggested for the bovine complex I [37,72], by a mechanism different from the reduction of FC, $APAD^+$, and oxygen [73]. The above is summarized in the form of a scheme of electron transfer by complex I from NADH to various electron acceptors, shown in Fig. 8 A. During forward electron transfer by complex I, there is only one electron input to the enzyme – reduction of FMN by NADH. In the absence of inhibitors electrons are transferred to ubiquinone and NADH:oxidase activity is catalyzed by the whole respiratory chain. Piericidin A inhibits that reaction by disrupting electron transfer to ubiquinone. When the respiration is inhibited, complex I is still capable of catalyzing electron transfer to artificial electron acceptors FC and HAR, to oxygen or to nucleotides. For all of these reactions FMN can serve as a primary electron donor and NADH-OH inhibits all of these NADH-dependent reactions catalyzed by complex I.

The most important finding reported in this paper is the NADH-OH-insensitive RET to HAR catalyzed by SBPs. During *pmf*-consuming RET, catalyzed by complex I, electron input is now located at the ubiquinone-binding site, hence, all of the RET activities are sensitive to both piericidin A and uncoupling. In the absence of inhibitors complex I reduces nucleotides (NAD^+, $APAD^+$), FC and oxygen in RET in *pmf*-dependent manner. NADH-OH is expected to be inhibitor for all RET reactions where FMN serves as an electron donor. Indeed, pyridine nucleotides, FC, and oxygen are not reduced by NADH-OH-inhibited complex I in RET (Table S1). The exception to this is RET to HAR which is insensitive to NADH-OH (see Fig. 6). From this follows that HAR could be reduced by complex I in an FMN-independent pathway, *i.e.*, there exists a non-FMN redox group of complex I capable of reducing HAR. This is corroborated by the complex kinetics of NADH:HAR-reductase activity of *P. denitrificans* SBPs, which also implies the existence of two different mechanisms of HAR reduction.

It's worth noting that the activity values for NADH-OH-insensitive RET to HAR are comparable to other RET activities catalyzed by SBPs and probably reflects the fact that maximal rate of ubiquinol oxidation by complex I is achieved. This suggests that the non-FMN electron donor to HAR is a competent one and is capable of supporting high steady-state turnover numbers. Insensitivity of RET to HAR to NADH-OH, catalyzed by *P. denitrificans* SBPs, corresponds well with our previous report of the same nature but observed with bovine heart SMPs [55] and shows that this is not exclusive for the mammalian enzyme but rather a common feature of complexes I from different species.

The exact physical nature of the hypothetical non-FMN electron donor to HAR is not established by us, but merits a quick discussion. HAR is a positively charged hydrophilic molecule with a radius of around 5 Å [74]. Its interaction with bovine complex I is insensitive to hexaamminecobalt (III) (unpublished result of this laboratory), so we assume that there is no special "site" for HAR reduction in the enzyme – the acceptor probably reacts by transient binding to a fitting protein surface. From this follows that HAR could react with complex I only at solvent-accessible areas that should preferably be negatively charged and in a close vicinity to one of the enzyme's redox groups. In most redox enzymes effective electron tunneling occurs at edge-to-edge distances between reacting centers of 14 Å or less but it is still possible even at larger distances, albeit with lower rates [75]. Recently in Sazanov's laboratory structures of *E. coli* complex I were determined in different conformations and to a sensational 2.3–2.5 Å resolutions [23]. This let authors to experimentally observe water molecules hydrating the enzyme and it turned out that water density in 10 Å radius around FeS clusters is very high [23]. This, coupled to the fact that there are large stretches of negatively-charged protein surfaces wrapping FeS clusters [23], suggests the possibility of protein backbone/water-assisted electron tunneling from FeS clusters to HAR. It is also well-known for a long time that complex I undergoes significant turnover-dependent [76], *pmf*-dependent [77], redox-dependent [53] or ligand binding-dependent [78,79] conformational changes in different areas of the enzyme that were shown by changes in tryptic digestion patterns [80], chemical cross-linking [81–84], cryo-EM structural studies [12,20,23,85,86] and other methods. This means that transient changes in the enzyme structure during turnover could provide for an opportunity of HAR diffusion closer to FeS clusters of complex I, so as to enable effective reduction of the acceptor. More studies are needed to definitively establish the nature of NADH-OH-insensitive electron donor for HAR in both bovine heart SMPs and *P. denitrificans* SBPs. Apparently, exact mechanism of NADH:HAR-reductase activity of the bacterial enzyme is also not fully understood.

It is hard to imagine, that only HAR would react with complex I in a NADH-OH-insensitive manner, albeit being the only substance to be shown to. Finding other chemicals that react with complex I in the same way could shed some light on this intriguing phenomenon. We also note that results presented here, and previously for the bovine enzyme [55], suggest that complex I could also be reduced by hydrophilic substances in NADH-OH-insensitive manner, potentially opening an interesting route of research.

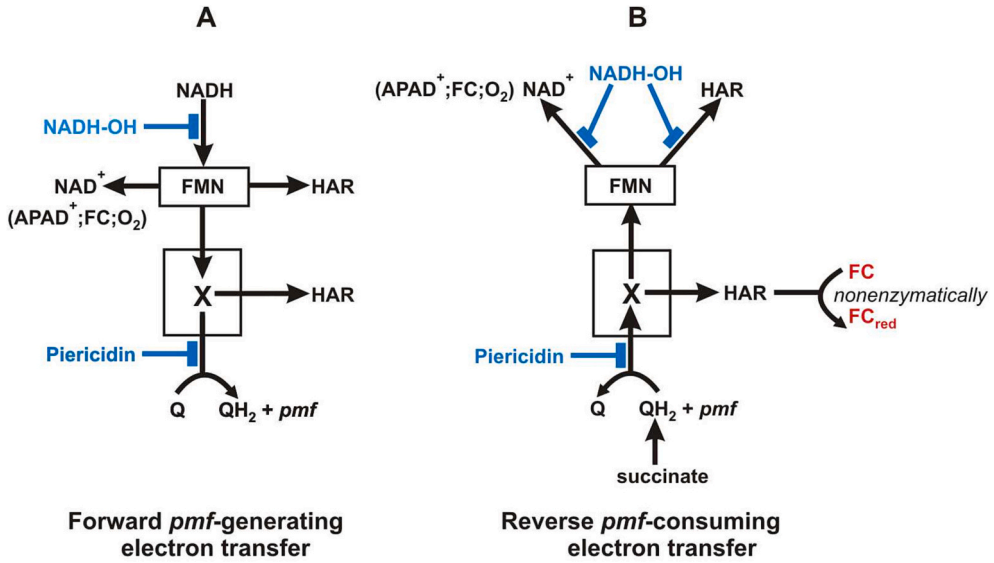

Fig. 8. Proposed scheme of electron-transfer pathways in complex I during forward (A) and reverse reactions (B). See text for explanation.

5. Conclusions

NADH-OH is shown to completely block FMN-dependent reactions of *P. denitrificans* complex I: NADH oxidation (in a competitive manner with K_i of 1 nM) as well as reduction of pyridine nucleotides, ferricyanide and oxygen in the reverse electron transfer.

A new assay procedure for measuring succinate-driven RET to HAR catalyzed by *P. denitrificans* SBPs is proposed. In contrast to all other activities checked, RET to HAR catalyzed by SBPs is insensitive to NADH-OH. This could be interpreted as the existence of a non-FMN redox group of *P. denitrificans* complex I that is capable of reducing HAR.

A scheme of electron-transfer pathways in complex I during forward and reverse reactions is proposed.

Kinetics of NADH:HAR-reductase reaction catalyzed by *P. denitrificans* SBPs is complex and follows different kinetic mechanisms depending on the concentrations of substrates used. Such kinetics corroborate the hypothesis of existence of a non-FMN electron donor for HAR in *P. denitrificans* complex I.

Declaration of competing interest

The authors declare that they have no known competing financial interests or personal relationships that could have appeared to influence the work reported in this paper.

Data availability

Data will be made available on request.

Acknowledgments

This study began under the guidance of prof. Andrei D. Vinogradov, who had headed our laboratory until 2020. We are eternally grateful to him for many years of collaborative work. This work is dedicated to his memory.

Funding

This work was supported by Russian Science Foundation (RSF) (grant number 22-24-00106, https://rscf.ru/en/project/22-24-00106).

CRediT authorship contribution statement

Grigory V. Gladyshev: Conceptualization, Methodology, Provision of study materials and reagents, Investigation, Formal analysis, Writing this article. **Tatyana V. Zharova:** Provision of study materials and reagents, Investigation. **Alexandra V. Kareyeva:** Provision of study materials and reagents, Investigation. **Vera G. Grivennikova:** Funding acquisition, Supervision, Conceptualization, Methodology, Investigation, Data curation, Formal analysis, Writing this article.

Ethics declarations

This article does not include the experiments involving humans or animals performed by any of the authors.

Appendix A. Supplementary data

Supplementary data to this article can be found online at https://doi.org/10.1016/j.bbabio.2023.148963.

References

[1] M. Wikström, Two protons are pumped from the mitochondrial matrix per electron transferred between NADH and ubiquinone, FEBS Lett. 169 (1984) 300–304, https://doi.org/10.1016/0014-5793(84)80338-5.

[2] A.S. Galkin, V.G. Grivennikova, A.D. Vinogradov, →H+/2ē stoichiometry in NADH-quinone reductase reactions catalyzed by bovine heart submitochondrial particles, FEBS Lett. 451 (1999) 157–161, https://doi.org/10.1016/S0014-5793(99)00575-X.

[3] V.G. Grivennikova, A.V. Ushakova, C. Hägerhäll, A.D. Vinogradov, Proton translocation catalyzed by paracoccus denitrificans NADH:quinone oxidoreductase (NDH-1), Biochim. Biophys. Acta EBEC Short Rep. 12 (2002) 208.

[4] S. Dröse, A. Galkin, U. Brandt, Proton pumping by complex I (NADH:ubiquinone oxidoreductase) from yarrowia lipolytica reconstituted into proteoliposomes, Biochim. Biophys. Acta - Bioenerg. 1710 (2005) 87–95, https://doi.org/10.1016/j.bbabio.2005.10.001.

[5] U. Weidner, S. Geier, A. Ptock, T. Friedrich, H. Leif, H. Weiss, The gene locus of the proton-translocating NADH: ubiquinone oxidoreductase in Escherichia coli: organization of the 14 genes and relationship between the derived proteins and subunits of mitochondrial complex I, J. Mol. Biol. 233 (1993) 109–122, https://doi.org/10.1006/jmbi.1993.1488.

[6] H. Leif, V.D. Sled, T. Ohnishi, H. Weiss, T. Friedrich, Isolation and characterization of the proton-translocating NADH:ubiquinone oxidoreductase from Escherichia coli, Eur. J. Biochem. 230 (1995) 538–548, https://doi.org/10.1111/j.1432-1033.1995.tb20594.x.

[7] T. Friedrich, K. Steinmüller, H. Weiss, The proton-pumping respiratory complex I of bacteria and mitochondria and its homologue in chloroplasts, FEBS Lett. 367 (1995) 107–111, https://doi.org/10.1016/0014-5793(95)00548-N.

[8] T. Yano, S.S. Chu, V.D. Sled', T. Ohnishi, T. Yagi, The proton-translocating NADH-quinone oxidoreductase (NDH-1) of thermophilic bacterium Thermus thermophilus HB-8 Complete DNA sequence of the gene cluster and thermostable properties of the expressed NQO2 subunit, J. Biol. Chem. 272 (1997) 4201–4211, https://doi.org/10.1074/jbc.272.7.4201.

[9] T. Yagi, T. Yano, S. Di Bernardo, A. Matsuno-Yagi, Procaryotic complex I (NDH-1) an overview, Biochim. Biophys. Acta - Bioenerg. 1364 (1998) 125–133, https://doi.org/10.1016/S0005-2728(98)00023-1.

[10] J. Carroll, I.M. Fearnley, J.M. Skehel, R.J. Shannon, J. Hirst, J.E. Walker, Bovine complex I is a complex of 45 different subunits, J. Biol. Chem. 281 (2006) 32724–32727, https://doi.org/10.1074/jbc.M607135200.

[11] E. Balsa, R. Marco, E. Perales-Clemente, R. Szklarczyk, E. Calvo, M.O. Landázuri, J. A. Enríquez, NDUFA4 is a subunit of complex IV of the mammalian electron transport chain, Cell Metab. 16 (2012) 378–386, https://doi.org/10.1016/j.cmet.2012.07.015.

[12] J. Zhu, K.R. Vinothkumar, J. Hirst, Structure of mammalian respiratory complex i, Nature 536 (2016) 354–358, https://doi.org/10.1038/nature19095.

[13] X. Xu, A. Matsuno-Yagi, T. Yagi, DNA sequencing of the seven remaining structural genes of the gene cluster encoding the energy-transducing NADH-quinone oxidoreductase of paracoccus denitrificans, Biochemistry 32 (1993) 968–981, https://doi.org/10.1021/bi00054a030.

[14] C.Y. Yip, M.E. Harbour, K. Jayawardena, I.M. Fearnley, L.A. Sazanov, Evolution of respiratory complex I "Supernumerary" subunits are present in the α-proteobacterial enzyme, J. Biol. Chem. 286 (2011) 5023–5033, https://doi.org/10.1074/jbc.M110.194993.

[15] T. Cremona, E.B. Kearney, Resolution of some problems concerning the reduced diphosphopyridine nucleotide dehydrogenase of the respiratory chain, Nature 200 (1963) 542–544, https://doi.org/10.1038/200542a0.

[16] T. Ohnishi, Iron-sulfur clusters/semiquinones in complex I, Biochim. Biophys. Acta - Bioenerg. 1364 (1998) 186–206, https://doi.org/10.1016/S0005-2728(98)00027-9.

[17] P. Hinchliffe, L.A. Sazanov, Organization of Iron-Sulfur Clusters in respiratory complex I, Science 309 (2005) 771–774, https://doi.org/10.1126/science.1113988.

[18] L.A. Sazanov, P. Hinchliffe, Structure of the hydrophilic domain of respiratory complex I from thermus thermophilus, Science 311 (2006) 1430–1436, https://doi.org/10.1126/science.1123809.

[19] H.R. Bridges, J.G. Fedor, J.N. Blaza, A. Di Luca, A. Jussupow, O.D. Jarman, J. J. Wright, A.-N.A. Agip, A.P. Gamiz-Hernandez, M.M. Roessler, V.R.I. Kaila, J. Hirst, Structure of inhibitor-bound mammalian complex I, Nat. Commun. 11 (2020) 5261, https://doi.org/10.1038/s41467-020-18950-3.

[20] K. Parey, J. Lasham, D.J. Mills, A. Djurabekova, O. Haapanen, E.G. Yoga, H. Xie, W. Kühlbrandt, V. Sharma, J. Vonck, V. Zickermann, High-resolution structure and dynamics of mitochondrial complex I—Insights into the proton pumping mechanism, Sci. Adv. 7 (2021) 1–12, https://doi.org/10.1126/sciadv.abj3221.

[21] P. Kolata, R.G. Efremov, Structure of escherichia coli respiratory complex i reconstituted into lipid nanodiscs reveals an uncoupled conformation, elife 10 (2021) 1–32, https://doi.org/10.7554/eLife.68710.

[22] I. Chung, J.J. Wright, H.R. Bridges, B.S. Ivanov, O. Biner, C.S. Pereira, G. M. Arantes, J. Hirst, Cryo-EM structures define ubiquinone-10 binding to mitochondrial complex I and conformational transitions accompanying Q-site occupancy, Nat. Commun. 13 (2022) 1–13, https://doi.org/10.1038/s41467-022-30506-1.

[23] V. Kravchuk, O. Petrova, D. Kampjut, A. Wojciechowska-Bason, Z. Breese, L. Sazanov, A universal coupling mechanism of respiratory complex I, Nature 609 (2022) 808–814, https://doi.org/10.1038/s41586-022-05199-7.

[24] A.-N.A. Agip, J.N. Blaza, J.G. Fedor, J. Hirst, Mammalian respiratory complex I through the lens of cryo-EM, Annu. Rev. Biophys. 48 (2019) 165–184, https://doi.org/10.1146/annurev-biophys-052118-115704.

[25] E. Galemou Yoga, H. Angerer, K. Parey, V. Zickermann, Respiratory complex I - mechanistic insights and advances in structure determination, Biochim. Biophys. Acta - Bioenerg. 1861 (2020), 148153, https://doi.org/10.1016/j.bbabio.2020.148153.

[26] D. Kampjut, L.A. Sazanov, Structure of respiratory complex I – an emerging blueprint for the mechanism, Curr. Opin. Struct. Biol. 74 (2022), 102350, https://doi.org/10.1016/j.sbi.2022.102350.
[27] A.H.V. Schapira, J.M. Cooper, D. Dexter, P. Jenner, J.B. Clark, C.D. Marsden, Mitochondrial complex i deficiency in PARKINSON'S disease, Lancet 333 (1989) 1269, https://doi.org/10.1016/S0140-6736(89)92366-0.
[28] J.T. Greenamyre, T.B. Sherer, R. Betarbet, A.V. Panov, Complex I and Parkinson's disease, IUBMB Life 52 (2001) 135–141, https://doi.org/10.1080/15216540152845939.
[29] R.J. Rodenburg, Mitochondrial complex I-linked disease, Biochim. Biophys. Acta - Bioenerg. 2016 (1857) 938–945, https://doi.org/10.1016/j.bbabio.2016.02.012.
[30] K. Fiedorczuk, L.A. Sazanov, Mammalian mitochondrial complex I structure and disease-causing mutations, Trends Cell Biol. 28 (2018) 835–867, https://doi.org/10.1016/j.tcb.2018.06.006.
[31] A. Galkin, Brain Ischemia/Reperfusion injury and mitochondrial complex I damage, Biochemist 84 (2019) 1411–1423, https://doi.org/10.1134/S0006297919110154.
[32] A.D. Vinogradov, NADH/NAD+ interaction with NADH: ubiquinone oxidoreductase (complex I), Biochim. Biophys. Acta - Bioenerg. 1777 (2008) 729–734, https://doi.org/10.1016/j.bbabio.2008.04.014.
[33] B. Chance, G. Hollunger, Energy-linked reduction of mitochondrial pyridine nucleotide, Nature 185 (1960) 666–672, https://doi.org/10.1038/185666a0.
[34] P.C. Hinkle, R.A. Butow, E. Racker, B. Chance, Partial resolution of the enzymes catalyzing oxidative phosphorylation XV reverse electron transfer in the flavin-cytochrome beta region of the respiratory chain of beef heart submitochondrial particles, J. Biol. Chem. 242 (1967) 5169–5173.
[35] A.B. Kotlyar, A.D. Vinogradov, Slow active/inactive transition of the mitochondrial NADH-ubiquinone reductase, BBA - Bioenerg. 1019 (1990) 151–158, https://doi.org/10.1016/0005-2728(90)90137-S.
[36] G. Dooijewaard, E.C. Slater, Steady-state kinetics of high molecular weight (type-I) NADH dehydrogenase, BBA - Bioenerg. 440 (1976) 1–15, https://doi.org/10.1016/0005-2728(76)90109-2.
[37] V.D. Sled, A.D. Vinogradov, Kinetics of the mitochondrial NADH-ubiquinone oxidoreductase interaction with hexammineruthenium(III), BBA - Bioenerg. 1141 (1993) 262–268, https://doi.org/10.1016/0005-2728(93)90051-G.
[38] E.V. Gavrikova, V.G. Grivennikova, V.D. Sled, T. Ohnishi, A.D. Vinogradov, Kinetics of the mitochondrial three-subunit NADH dehydrogenase interaction with hexammineruthenium(III), BBA - Bioenerg. 1230 (1995) 23–30, https://doi.org/10.1016/0005-2728(95)00015-B.
[39] M. Gutman, T.P. Singer, H. Beinert, J.E. Casida, Reaction sites of rotenone, piericidin a, and amytal in relation to the nonheme iron components of NADH dehydrogenase, Proc. Natl. Acad. Sci. U. S. A. 65 (1970) 763–770, https://doi.org/10.1073/pnas.65.3.763.
[40] G. Dooijewaard, E.C. Slater, Steady-state kinetics of low molecular weight (type-II) NADH dehydrogenase, BBA - Bioenerg. 440 (1976) 16–35, https://doi.org/10.1016/0005-2728(76)90110-9.
[41] S. Minakami, T. Cremona, R.L. Ringler, T.P. Singer, Studies on the respiratory chain-linked reduced nicotinamide adenine dinucleotide dehydrogenase III catalytic properties of the enzyme from beef heart, J. Biol. Chem. 238 (1963) 1529–1537.
[42] V. Zickermann, S. Kurki, M. Kervinen, I. Hassinen, M. Finel, The NADH oxidation domain of complex I: do bacterial and mitochondrial enzymes catalyze ferricyanide reduction similarly? Biochim. Biophys. Acta - Bioenerg. 1459 (2000) 61–68, https://doi.org/10.1016/S0005-2728(00)00113-4.
[43] A.D. Vinogradov, V.G. Grivennikova, Oxidation of NADH and ROS production by respiratory complex i, Biochim. Biophys. Acta - Bioenerg. 2016 (1857) 863–871, https://doi.org/10.1016/j.bbabio.2015.11.004.
[44] V.G. Grivennikova, R. Roth, N.V. Zakharova, C. Hägerhäll, A.D. Vinogradov, The mitochondrial and prokaryotic proton-translocating NADH:ubiquinone oxidoreductases: similarities and dissimilarities of the quinone-junction sites, Biochim. Biophys. Acta - Bioenerg. 1607 (2003) 79–90, https://doi.org/10.1016/j.bbabio.2003.09.001.
[45] V.G. Grivennikova, G.V. Gladyshev, A.D. Vinogradov, Allosteric nucleotide-binding site in the mitochondrial NADH:ubiquinone oxidoreductase (respiratory complex I), FEBS Lett. 585 (2011) 2212–2216, https://doi.org/10.1016/j.febslet.2011.05.039.
[46] A.D. Vinogradov, Kinetics, control, and mechanism of ubiquinone reduction by the mammalian respiratory chain-linked NADH-ubiquinone reductase, J. Bioenerg. Biomembr. 25 (1993) 367–375, https://doi.org/10.1007/BF00762462.
[47] A.D. Vinogradov, Catalytic properties of the mitochondrial NADH–ubiquinone oxidoreductase (Complex I) and the pseudo-reversible active/inactive enzyme transition, Biochim. Biophys. Acta - Bioenerg. 1364 (1998) 169–185, https://doi.org/10.1016/S0005-2728(98)00026-7.
[48] A.D. Vinogradov, V.G. Grivennikova, The mitochondrial complex I: Progress in understanding of catalytic properties, IUBMB Life 52 (2001) 129–134, https://doi.org/10.1080/15216540152845920.
[49] M. Degli Esposti, Inhibitors of NADH-ubiquinone reductase: an overview, Biochim. Biophys. Acta - Bioenerg. 1364 (1998) 222–235, https://doi.org/10.1016/S0005-2728(98)00029-2.
[50] M. Murai, H. Miyoshi, Current topics on inhibitors of respiratory complex i, Biochim. Biophys. Acta - Bioenerg. 2016 (1857) 884–891, https://doi.org/10.1016/j.bbabio.2015.11.009.
[51] T.V. Zharova, A.D. Vinogradov, A competitive inhibition of the mitochondrial NADH-ubiquinone oxidoreductase (Complex I) by ADP-ribose, Biochim. Biophys. Acta - Bioenerg. 1320 (1997) 256–264, https://doi.org/10.1016/S0005-2728(97)00029-7.
[52] A.B. Kotlyar, J.S. Karliner, G. Cecchini, A novel strong competitive inhibitor of complex I, FEBS Lett. 579 (2005) 4861–4866, https://doi.org/10.1016/j.febslet.2005.07.076.
[53] V.G. Grivennikova, A.B. Kotlyar, J.S. Karliner, G. Cecchini, A.D. Vinogradov, Redox-dependent change of nucleotide affinity to the active site of the mammalian complex I, Biochemistry 46 (2007) 10971–10978, https://doi.org/10.1021/bi7009822.
[54] M. Vranas, D. Wohlwend, D. Qiu, S. Gerhardt, C. Trncik, M. Pervaiz, K. Ritter, S. Steimle, A. Randazzo, O. Einsle, S. Günther, H.J. Jessen, A. Kotlyar, T. Friedrich, Structural basis for inhibition of ROS-producing respiratory complex I by NADH-OH, Angew. Chem. Int. Ed. 60 (2021) 27277–27281, https://doi.org/10.1002/anie.202112165.
[55] G.V. Gladyshev, V.G. Grivennikova, A.D. Vinogradov, FMN site-independent energy-linked reverse electron transfer in mitochondrial respiratory complex I, FEBS Lett. 592 (2018) 2213–2219, https://doi.org/10.1002/1873-3468.13117.
[56] P. John, F.R. Whatley, Oxidative phosphorylation coupled to oxygen uptake and nitrate reduction in Micrococcus denitrificans, BBA - Bioenerg. 216 (1970) 342–352, https://doi.org/10.1016/0005-2728(70)90225-2.
[57] P. John, W.A. Hamilton, Respiratory control in membrane particles from Micrococcus denitrificans, FEBS Lett. 10 (1970) 246–248, https://doi.org/10.1016/0014-5793(70)80639-1.
[58] V.G. Grivennikova, G.V. Gladyshev, A.D. Vinogradov, Deactivation of mitochondrial NADH:ubiquinone oxidoreductase (respiratory complex I): extrinsically affecting factors, Biochim. Biophys. Acta - Bioenerg. 1861 (2020), 148207, https://doi.org/10.1016/j.bbabio.2020.148207.
[59] V.G. Grivennikova, D.V. Serebryanaya, E.P. Isakova, T.A. Belozerskaya, A. D. Vinogradov, The transition between active and de-activated forms of NADH: ubiquinone oxidoreductase (Complex I) in the mitochondrial membrane of neurospora crassa, Biochem. J. 369 (2003) 619–626, https://doi.org/10.1042/bj20021165.
[60] M. Zhou, Z. Diwu, N. Panchuk-Voloshina, R.P. Haugland, A stable nonfluorescent derivative of resorufin for the fluorometric determination of trace hydrogen peroxide: applications in detecting the activity of phagocyte NADPH oxidase and other oxidases, Anal. Biochem. 253 (1997) 162–168, https://doi.org/10.1006/abio.1997.2391.
[61] V.G. Grivennikova, A.V. Kareyeva, A.D. Vinogradov, Oxygen-dependence of mitochondrial ROS production as detected by amplex red assay, Redox Biol. 17 (2018) 192–199, https://doi.org/10.1016/j.redox.2018.04.014.
[62] F. Pacheco-Moisés, J.J. Garcia, J.S. Rodríguez-Zavala, R. Moreno-Sánchez, Sulfite and membrane energization induce two different active states of the paracoccus denitrificans F0F1-ATPase, Eur. J. Biochem. 267 (2000) 993–1000, https://doi.org/10.1046/j.1432-1327.2000.01088.x.
[63] T.V. Zharova, A.D. Vinogradov, Proton-translocating ATP-synthase of paracoccus denitrificans: ATP-hydrolytic activity, Biochemistry (Mosc) 68 (2003) 1101–1108, https://doi.org/10.1023/a:1026306611821.
[64] V.G. Grivennikova, E.O. Maklashina, E.V. Gavrikova, A.D. Vinogradov, Interaction of the mitochondrial NADH-ubiquinone reductase with rotenone as related to the enzyme active/inactive transition, Biochim. Biophys. Acta - Bioenerg. 1319 (1997) 223–232, https://doi.org/10.1016/S0005-2728(96)00163-6.
[65] R.A. Scott, H.B. Gray, Cytochrome aa3 electron-transfer reactions kinetics of hexaammineruthenium(II) reduction of the beef heart enzyme, J. Am. Chem. Soc. 102 (1980) 3219–3224, https://doi.org/10.1021/ja00529a054.
[66] J.H. Hochman, B. Partridge, S. Ferguson-miller, An effective electron donor to cytochrome oxidase, J. Biol. Chem. 256 (1981) 8693–8698.
[67] V. Zickermann, C. Wirth, H. Nasiri, K. Siegmund, H. Schwalbe, C. Hunte, U. Brandt, Mechanistic insight from the crystal structure of mitochondrial complex I, Science 347 (2015) 44–49, https://doi.org/10.1126/science.1259859.
[68] T. Yano, V.D. Sled, T. Ohnishi, T. Yagi, Expression and characterization of the flavoprotein subcomplex composed of 50-kDa (NQO1) and 25-kDa (NQO2) subunits of the proton-translocating NADH-quinone oxidoreductase of paracoccus denitrificans, J. Biol. Chem. 271 (1996) 5907–5913, https://doi.org/10.1074/jbc.271.10.5907.
[69] V.D. Sled, N.I. Rudnitzky, T. Ohnishi, Y. Hatefi, Thermodynamic analysis of flavin in mitochondrial NADH: ubiquinone oxidoreductase (Complex I), Biochemistry 33 (1994) 10069–10075, https://doi.org/10.1021/bi00199a034.
[70] K.R. Pryde, J. Hirst, Superoxide is produced by the reduced flavin in mitochondrial complex I: a single, unified mechanism that applies during both forward and reverse electron transfer, J. Biol. Chem. 286 (2011) 18056–18065, https://doi.org/10.1074/jbc.M110.186841.
[71] T. Yano, J. Sklar, E. Nakamaru-Ogiso, Y. Takahashi, T. Yagi, T. Ohnishi, Characterization of cluster N5 as a fast-relaxing [4Fe-4S] cluster in the Nqo3 subunit of the proton-translocating NADH-ubiquinone oxidoreductase from paracoccus denitrificans, J. Biol. Chem. 278 (2003) 15514–15522, https://doi.org/10.1074/jbc.M212275200.
[72] J.A. Birrell, M.S. King, J. Hirst, A ternary mechanism for NADH oxidation by positively charged electron acceptors, catalyzed at the flavin site in respiratory complex i, FEBS Lett. 585 (2011) 2318–2322, https://doi.org/10.1016/j.febslet.2011.05.065.
[73] J.A. Birrell, G. Yakovlev, J. Hirst, Reactions of the flavin mononucleotide in complex I: a combined mechanism describes NADH oxidation coupled to the reduction of APAD+, ferricyanide, or molecular oxygen, Biochemistry 48 (2009) 12005–12013, https://doi.org/10.1021/bi901706w.
[74] H.C. Stynes, J.A. Ibers, Effect of metal-ligand bond distances on rates of electron-transfer reactions crystal structures of hexaammineruthenium(II) iodide, [Ru(NH3)6]I2, and hexaammineruthenium(III) tetrafluoroborate, [Ru(NH3)6][BF4]3, Inorg. Chem. 10 (1971) 2304–2308, https://doi.org/10.1021/ic50104a043.

[75] P.L. Dutton, C.C. Mosser, Quantum biomechanics of long-range electron transfer in protein: hydrogen bonds and reorganization energies, Proc. Natl. Acad. Sci. U. S. A. 91 (1994) 10247–10250, https://doi.org/10.1073/pnas.91.22.10247.
[76] A. Galkin, B. Meyer, I. Wittig, M. Karas, H. Schägger, A. Vinogradov, U. Brandt, Identification of the mitochondrial ND3 subunit as a structural component involved in the active/deactive enzyme transition of respiratory complex I, J. Biol. Chem. 283 (2008) 20907–20913, https://doi.org/10.1074/jbc.M803190200.
[77] A.M.P. de Jong, A.B. Kotlyar, S.P.J. Albracht, Energy-induced structural changes in NADH: Q oxidoreductase of the mitochondrial respiratory chain, BBA - Bioenerg. 1186 (1994) 163–171, https://doi.org/10.1016/0005-2728(94)90175-9.
[78] R. Hielscher, T. Friedrich, P. Hellwig, Far- and mid-infrared spectroscopic analysis of the substrate-induced structural dynamics of respiratory complex I, ChemPhysChem 12 (2011) 217–224, https://doi.org/10.1002/cphc.201000688.
[79] M. Verkhovskaya, N. Belevich, Fluorescent signals associated with respiratory complex i revealed conformational changes in the catalytic site, FEMS Microbiol. Lett. 366 (2019) 1–7, https://doi.org/10.1093/femsle/fnz155.
[80] M. Yamaguchi, G.I. Belogrudov, Y. Hatefi, Mitochondrial NADH-ubiquinone oxidoreductase (Complex I) effect of substrates on the fragmentation of subunits by trypsin, J. Biol. Chem. 273 (1998) 8094–8098, https://doi.org/10.1074/jbc.273.14.8094.
[81] G. Belogrudov, Y. Hatefi, Catalytic sector of complex I (NADH: ubiquinone Oxidoreductase): subunit stoichiometry and substrate-induced conformation changes, Biochemistry 33 (1994) 4571–4576, https://doi.org/10.1021/bi00181a018.
[82] A.A. Mamedova, P.J. Holt, J. Carroll, L.A. Sazanov, Substrate-induced conformational change in bacterial complex I, J. Biol. Chem. 279 (2004) 23830–23836, https://doi.org/10.1074/jbc.M401539200.
[83] J.M. Berrisford, C.J. Thompson, L.A. Sazanov, Chemical and NADH-induced, ROS-dependent, cross-linking between subunits of complex I from Escherichia coli and thermus thermophilus, Biochemistry 47 (2008) 10262–10270, https://doi.org/10.1021/bi801160u.
[84] M. Babot, P. Labarbuta, A. Birch, S. Kee, M. Fuszard, C.H. Botting, I. Wittig, H. Heide, A. Galkin, ND3, ND1 and 39 kDa subunits are more exposed in the de-active form of bovine mitochondrial complex I, Biochim. Biophys. Acta - Bioenerg. 2014 (1837) 929–939, https://doi.org/10.1016/j.bbabio.2014.02.013.
[85] A.-N.A. Agip, J.N. Blaza, H.R. Bridges, C. Viscomi, S. Rawson, S.P. Muench, J. Hirst, Cryo-EM structures of complex I from mouse heart mitochondria in two biochemically defined states, Nat. Struct. Mol. Biol. 25 (2018) 548–556, https://doi.org/10.1038/s41594-018-0073-1.
[86] D. Kampjut, L.A. Sazanov, The coupling mechanism of mammalian respiratory complex I, Science 370 (2020), eabc4209, https://doi.org/10.1126/science.abc4209.